

## DETECTION OF FLOW MALDISTRIBUTION IN TRICKLE-BED REACTORS VIA TRACERS

P. J. HANRATTY and M. P. DUDUKOVIĆ<sup>†</sup>

Chemical Reaction Engineering Laboratory, Washington University, St. Louis, MO 63130, U.S.A.

(First received 23 August 1991; accepted in revised form 17 December 1991)

**Abstract**—Impulse tracer response curves are often used to assess flow distribution within a reactor. For a trickle-bed (and single-phase flow packed-bed) reactor, such a response curve represents both the flowing fluid and the fluid trapped in the porous packing. This makes the assessment of the needed flow distribution external to the particles difficult. A method for decoupling the particle effects from the tracer response curve was introduced recently by Hanratty and Duduković. This method showed promise based on computer-simulated data. The scope of this study was to critically evaluate this method by applying it to actual experimental data, and to determine the range of its validity. The results show that this method, which requires the use of tracers of different adsorptivity, can successfully distinguish between well-distributed reactors, for which the impulse response of the fluid external to the particles is obtained, and maldistributed reactors, for which maldistribution is identified but not quantified.

### INTRODUCTION

Trickle beds, and packed beds with single-phase flow, sometimes operate at lower than expected conversion or yield. It is important to assess whether this reduced reactor performance is caused by flow maldistribution or by particle-scale events, such as catalyst deactivation. For that purpose, impulse tracer studies are most often conducted. Other methods for the detection of flow maldistribution are available, but often require special sensors [e.g. Sapre *et al.* (1990) used a heater probe technique]. This paper focusses on perhaps the most popular method which is tracer studies. A slug of tracer (a detectable fluid whose properties are similar to those of the flowing fluid) is injected into the reactor inlet stream and the tracer concentration of the reactor effluent is monitored vs time. The normalized tracer impulse response curve,  $E_i(t)$ , results from such a tracer study. The  $E_i(t)$  curve gives an indication of the fluid history in the reactor from which the flow distribution in the reactor can be deduced.

For a trickle-bed reactor, the  $E_i(t)$  curve reflects the combined history of the tracer in the flowing fluid external to the particles and its sojourn in the porous particles. However, the extent of maldistribution (i.e. the departure from plug-flow behavior for which trickle beds are designed) only can be accurately determined from the impulse response of a tracer that does not penetrate the particle pore structure, and hence traces only the fluid external to the particles,  $E_{ext}(t)$ . Such a tracer is hard to find in practice. Particle-tracer interactions (i.e. diffusion into the particles and adsorption to the particle surface) broaden the tracer response curve (causing an increased variance) and shift the centroid (mean residence time) of the tracer response to longer times. These effects often mask the maldistribution of the flowing fluid in the observed tracer response curve. Methods currently

used to extract information about maldistribution from tracer responses [analysis of variance (Schneider and Smith, 1968)], intensity function (Naor and Shinnar, 1963)], and the cumulative residence-time distribution function [Robinson and Tester (1986)] are best applied to  $E_{ext}(t)$ .

Hanratty and Duduković (1990) outlined a method, called the Laplace transform (LT) method, by which the particle effect can be decoupled from the tracer impulse response curve,  $E_i(t)$ , leading to the impulse response curve of the flowing fluid external to the particles,  $E_{ext}(t)$ . Using model-generated data only, they demonstrated the robustness of the method for well-distributed and maldistributed reactors in the presence of simulated experimental error. In this paper, the LT method is applied, for the first time, to actual experimental tracer data from both well-distributed and maldistributed trickle-bed reactors. Such a treatment of actual data is essential to test the validity and potential usefulness of the LT method.

### DEVELOPMENT OF THE LT METHOD

To decouple the particle and flowing fluid effects, the bulk flowing fluid and the particle phase are represented by two regions which communicate with each other through a mass transfer or exchange coefficient. The mass transfer flux is the product of the exchange (mass transfer) coefficient and the difference between the bulk tracer concentration in the vicinity of the particle and the outside surface concentration of the tracer on the particle. Since the particle characteristic length is much smaller than the characteristic reactor length, it is reasonable to assume that the tracer enters and leaves the particle at the same axial point in the reactor. Mathematically, this implies that the covariance of the joint probability density function for the tracer sojourn in the particles and in the external fluid is zero (Aris, 1982). Under such assumptions, for a nonvolatile tracer that diffuses, and

<sup>†</sup>Author to whom correspondence should be addressed.

perhaps adsorbs, in the particles, the following differential equation for the LT of the point concentration of the *i*th tracer can be written (Duduković, 1986):

$$L(\bar{C}_i) = \varepsilon_L [s + k_{ex,i} H_i(s)/\varepsilon_L] \bar{C}_i \quad (1)$$

where  $\bar{C}_i$  is the LT of the tracer concentration,  $\varepsilon_L$  is the external liquid holdup,  $k_{ex,i}$  is the exchange coefficient between the flowing fluid and the particles for the *i*th tracer,  $H_i(s)$  is the tracer-dependent particle transfer function which incorporates the effective diffusivity,  $D_{eff,i}$ , and adsorption equilibrium constant,  $K_{a,i}$ , for the *i*th tracer,  $L(\cdot)$  is a linear operator describing the flow field external to the particles, and  $s$  is the argument of the LT with respect to time.

Now consider the case of an injected pulse of tracer that does not interact with the particle and flows only with the fluid external to the particles. In practice, such a tracer is hard to find, but it represents a useful case for understanding the development of this method. A mass balance over the tracer in the flow region yields

$$L(\bar{C}_i) = \varepsilon_L p \bar{C}_i \quad (2)$$

where  $p$  is now used as the argument of the LT. Comparing eqs (1) and (2),  $p$  and  $s$  can be related by the following equation:

$$p = s + k_{ex,i} H_i(s)/\varepsilon_L \quad (3)$$

and the equation for  $E_{ext}(t)$  can be written as

$$E_{ext}(t) = \mathcal{L}^{-1} \left( \int_0^{\infty} E_i(t) \exp \left\{ -[s - k_{ex,i} H_i(s)/\varepsilon_L] t \right\} dt \right) \quad (4)$$

where  $\mathcal{L}^{-1}$  is the inverse Laplace operation.

Based on the above development, the following procedure, illustrated in Fig. 1, was adopted to obtain  $E_{ext}(t)$  from the tracer response curve for the reactor: (a) determine the normalized impulse response curve of the *i*th tracer,  $E_i(t)$ ; (b) transform the tracer response curve into the Laplace domain [ $\bar{E}_i(s) = \int_0^{\infty} E_i(t) \exp(-st) dt$ ]; (c) shift the Laplace variable by eq. (3) [i.e.  $p = s + k_{ex,i} H_i(s)/\varepsilon_L$ ], and (d) invert the resulting LT into the time domain to obtain  $E_{ext}(t)$ . If

$N$  impulse tracer studies are conducted with  $N$  different tracers,  $N$  different tracer response curves, corresponding to Fig. 1(a), will be obtained. The resulting  $E_{ext}(t)$  curve, after applying the LT method, should be the same for all  $N$  tracers, corresponding to Fig. 1(d).

The development (and choice) of a particle transfer function is important to implement this procedure. Beaudry (1986) has shown that the following particle transfer function can be used for a partially internally and externally wetted sphere:

$$H_i(s) = \left\{ 1 + \frac{Bi}{\Phi_T} \left[ \frac{1}{\coth(3\Phi_1)} - 1/(3\Phi_1) \right] \right\}^{-1} \quad (5)$$

with

$$Bi = \frac{k_{LS} V_p}{D_{eff} S_x} \quad (6)$$

$$\Phi_T = \frac{V_p}{S_x} \left[ \frac{\varepsilon_p S_x}{D_{eff}} (1 + K_{ad} \rho_p / \varepsilon_p) \right]^{1/2} \quad (7)$$

$$\Phi_1 = \Phi_T \eta_{el} / \eta_{e_x} \quad (8)$$

where  $V_p$  and  $S_x$  are the volume and external area of the particle, respectively,  $\eta_{el}$  and  $\eta_{e_x}$  are the internal and external particle wetting efficiencies,  $\varepsilon_p$  is the particle porosity,  $\rho_p$  is the particle density,  $k_{LS}$  is the liquid-solid mass transfer coefficient,  $D_{eff}$  is the effective diffusivity, and  $K_{ad}$  is the adsorption equilibrium constant. Other particle transfer functions, useful for trickle-bed reactors, are given by Beaudry (1986) and by Ramachandran and Smith (1982).

## EXPERIMENTAL

A schematic of the experimental apparatus which was used to conduct the impulse tracer studies is illustrated in Fig. 2. The reactor column is shown in the middle of the schematic. The equipment to the right of the reactor column represents the gas delivery system. The equipment to the left of the reactor column represents the liquid delivery system. The measuring and data acquisition system is shown below the column. The tracer injection port is shown above the column. Details of such a setup for tracer studies are provided by Mills and Duduković (1981) and Hanratty (1988).

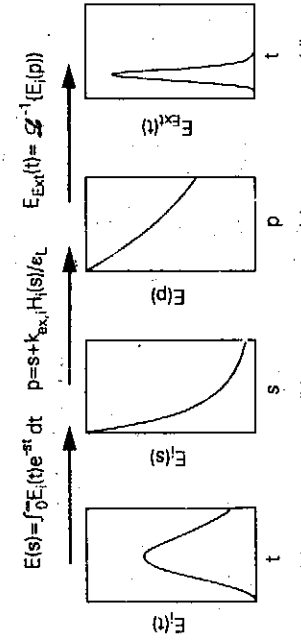


Fig. 1. Procedure for decoupling the external fluid impulse response from the overall tracer impulse response by the LT method.

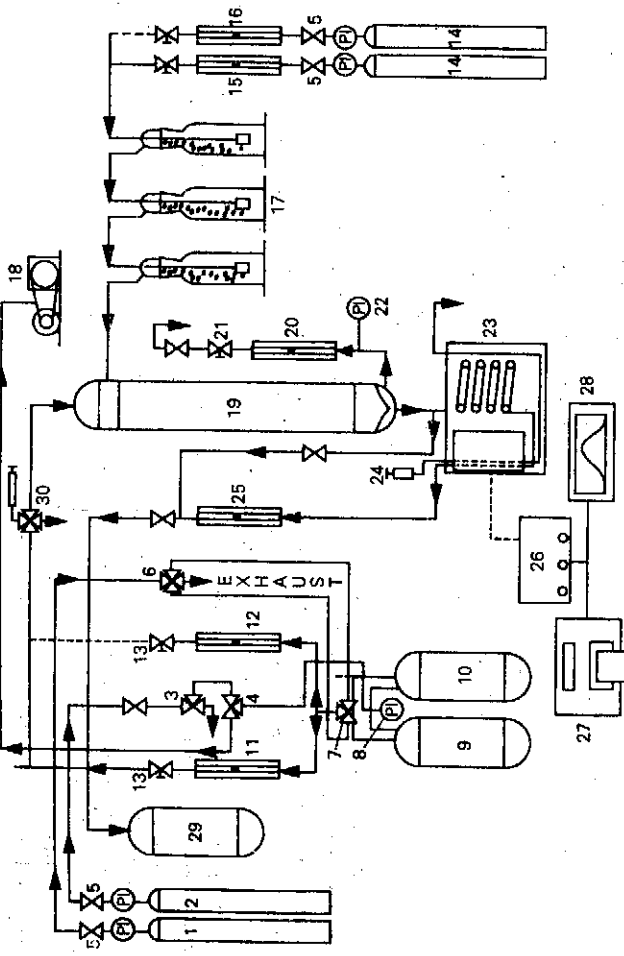


Fig. 2. Schematic of the experimental apparatus.

The reactor was a borosilicate glass tube with an i.d. of 1.905 cm and an overall length of 35 cm. The reactor tube was constructed so that different reactor heads could be used with it. Different reactor heads allow the reactor to be configured for liquid or gas-liquid flow experiments. The liquid and gas were distributed over the packing using either a fritted glass disk or a fritted glass bulb.

The impulse tracer disturbances were injected using a six-port chromatographic sampling valve. The sampling valve was equipped with a 0.5 and a 1.0 ml sampling loop which was used to introduce the impulse tracer disturbance into the input liquid line.

At the reactor exit, the liquid and gas are separated. The liquid stream is sent to an analytical unit. The gas stream is sent either to the hood or to a gas chromatograph. The tracer concentration in the effluent liquid stream was continuously measured with a Waters R403 flow-through differential refractometer. This unit continuously measures the refractive index of the effluent liquid, which is proportional to the tracer concentration. The data from the refractometer was sampled and recorded using an Apple II data acquisition system.

The LT method was experimentally investigated for both a well-distributed and a purposely maldistributed reactor. A maldistributed reactor was obtained by tilting the reactor 10° from the vertical axis. Such tilting causes the liquid to flow preferentially in the lower portion of the bed due to gravity. This is known to cause gross liquid bypassing (maldistribution).

To account for the liquid volume external to the reactor bed which is traversed by the tracer between

the injection port and the refractometer, tracer studies were conducted with the reactor bed removed and the two reactor heads (reactor entrance and exit) connected together. Assuming that the system is linear, the tracer response curve for the bed, or reactor tracer response,  $E_i(t)$ , can be determined by deconvolution of the tracer response curve for the entire system or overall tracer response,  $E_{\text{tot},i}(t)$ , and the tracer response curve for the system with the bed removed,  $E_{\text{ws},i}(t)$ . Deconvolution corresponds to the following division in the Laplace domain of the corresponding transforms:

$$\bar{E}_i(s) = \frac{\bar{E}_{\text{tot},i}(s)}{\bar{E}_{\text{ws},i}(s)}. \quad (9)$$

Since the response curve for the system with the bed removed is independent of the tracer, the externals were characterized with a single tracer at each of the gas-liquid flow rates used.

Properties of the catalyst packing are listed in Table 1. Hexane (liquid) and nitrogen (gas) were used as the carrier fluids for the two-phase flow experiments. The tracers used were heptane, cyclohexene and benzene. These tracers have different adsorptivities and effective diffusion coefficients in catalyst particles as seen in Table 2. Tracer experiments were conducted at liquid flow rates of 0.158–0.5 cm<sup>3</sup>/s and gas flow rates of 0.0–0.8 cm<sup>3</sup>/s at STP. The reactor temperature was 25°C and the pressure was 1 atm.

The tracer-particle parameters needed to apply the LT method are shown in Table 2. The liquid-solid contacting efficiency  $\eta_e$  (i.e. the fraction of the external area of the particles covered by liquid) was

calculated from the correlation of El-Hisnawi *et al.* (1982) which is also reported by Beaudry *et al.* (1987). The liquid-solid mass transfer coefficient for single-phase flow was calculated from a correlation of Dwivedi and Upadhyay (1977). For two-phase flow experiments, the correlation of Tan and Smith (1982) is used. The effective diffusivity,  $D_{eff}$ , and the adsorption equilibrium coefficient,  $K_a$ , were estimated for each tracer from the experimentally measured tracer response curves in a liquid full column (liquid flow only). The values for  $K_a$  and  $D_{eff}$  should be the same for both liquid and liquid-gas flow over the packing. The adsorption equilibrium constant was calculated from the first moment of the tracer response curve and the effective diffusivity from the slope of the variance of the tracer response curve plotted vs the liquid flow rate. Both methods were illustrated by Mills and Dudukovic (1981). A more detailed description of the determination of these parameters is given by Hanratty (1988). The parameter values, obtained as described above, were then utilized to test the LT method for two-phase flow experiments.

#### RESULTS AND DISCUSSION

The method was first investigated experimentally for a reactor operating under normal conditions (well-distributed). Tracer experiments were conducted using all three tracers (heptane, cyclohexene and benzene) at a number of different liquid (0.158–0.5 cm<sup>3</sup>/s) and gas flow rates (0.0–8.0 cm<sup>3</sup>/s at STP) which are all in the trickle-flow regime. These flow rates ensured contacting efficiencies in the range 0.8–1. The LT method was applied to the impulse tracer response curves obtained at each of the different flow conditions. For each set of gas and liquid flow rates, a nearly identical  $E_{out}(t)$  was produced by the LT method for each of the three tracers, although the original tracer impulse responses,  $E_i(t)$ , for the three tracers are very different.

To illustrate the results of the method, Fig. 3 shows the actual voltage (output from the differential

refractometer which is proportional to the tracer concentration) vs time for the three tracers at a liquid flow rate of 0.158 cm<sup>3</sup>/s and a gas flow rate of 3.5 cm<sup>3</sup>/s (at STP).

Figure 4 shows the normalized impulse overall tracer response of the reactor system and auxiliary lines for each of the three tracers,  $E_{out,i}(t)$ . Figure 5 illustrates the response curve of the volume external to the reactor bed,  $E_{ext}(t)$ . The LT method was applied to the reactor impulse response obtained by deconvoluting via eq. (9) the overall response curve, shown in Fig. 4, and the responses of the externals, shown in Fig. 5. Since the operations for the LT method are conducted in the Laplace domain,

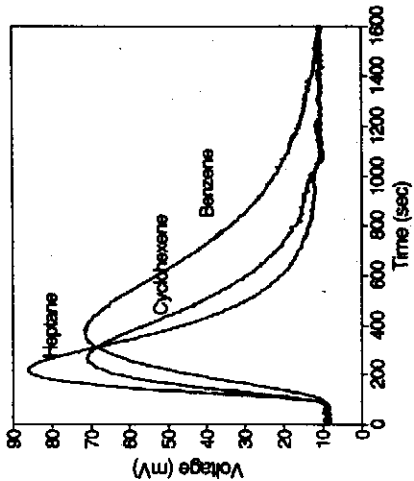


Fig. 3. Refractometer output voltage for the three tracers at a liquid flow rate of 0.158 cm<sup>3</sup>/s and a gas flow rate of 3.5 cm<sup>3</sup>/s (STP).

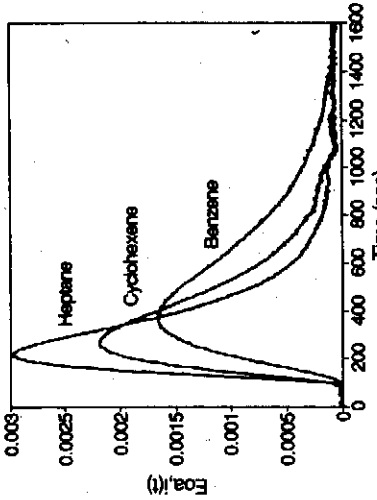


Fig. 4. Normalized impulse responses,  $E_i(t)$ , for data of Fig. 3.

Table 2. Particle transfer function parameters

Property	Heptane	Cyclohexene	Benzene
$k_{LS}$ (cm/s)	$1.05 \times 10^{-3}/\eta_{ee}$	$1.18 \times 10^{-3}/\eta_{ee}$	$1.19 \times 10^{-3}/\eta_{ee}$
$\rho_p K_a$	0.0	0.185	0.325
$D_{eff}$ (cm <sup>2</sup> /s)	$4.94 \times 10^{-6}$	$5.96 \times 10^{-6}$	$7.39 \times 10^{-6}$
Surface area (m <sup>2</sup> /g)	400.0		

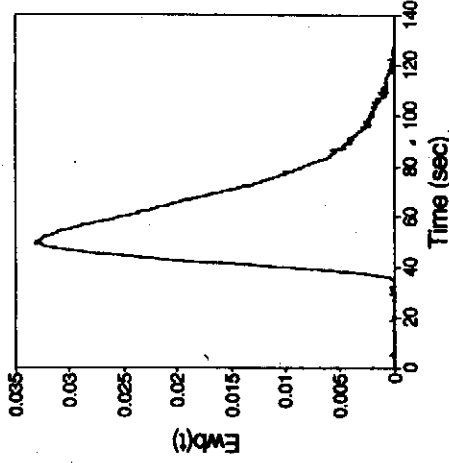


Fig. 5. Normalized impulse response for the volume external to the packed column.

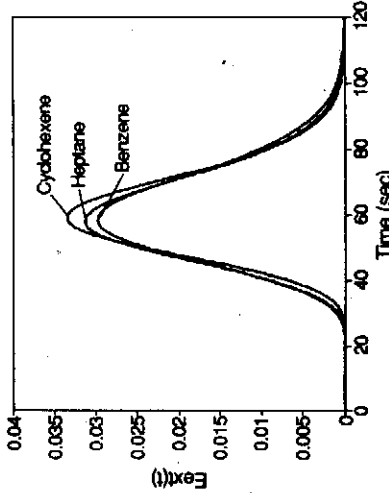


Fig. 6. External impulse responses,  $E_{ext}(t)$ , predicted by the LT method for the tracer curves of Fig. 4 (normal operation).

only the LTs of the reactor responses were generated. The particle transfer function described by eqs (5)-(8) (partially wetted sphere) was used. The particle transfer function parameters needed are listed in Tables 1 and 2. Figure 6 shows the  $E_{ext}(t)$  extracted for each tracer by the LT method. All three tracers of different adsorptivity, upon application of the LT method, yield the same impulse response of the fluid external to particles,  $E_{ext}(t)$ . The shape of this curve, its mean and variance, are almost the same for each tracer. The small differences are caused by parameter uncertainty or numerically induced errors. Visual inspection of  $E_{ext}(t)$  indicates absence of maldistribution. Absence of maldistribution can be readily confirmed by the variance test (Schneider and Smith, 1968), or by the intensity function (Naor and Shinnar, 1963) based on  $E_{ext}(t)$ . This fact that a single  $E_{ext}(t)$  is obtained from different experimental tracer responses in a nonmaldistributed reactor confirms our previous conclusions which are based on numerical simulations (Hanratty and Duduković, 1990).

One should note that the mean residence times of the three tracers in the external fluid are very similar: 60.6 s for hexane, 61.2 s for cyclohexene, and 61.2 s for benzene. This corresponds to an external liquid holdup of about 0.13 which is equal to the value calculated for the external holdup from the tracer response curves in Figs 4 and 5 assuming complete internal wetting of the particles. Similar results were obtained at all liquid flow rates. For each of these cases, no maldistribution was detected and the liquid was always close to plug flow.

After testing the LT method for a laboratory trickle bed under normal conditions of good liquid distribution (at near plug flow), the method was experimentally tested for a purposely maldistributed reactor. As stated before, the reactor was maldistributed by tilting the column 10° off the vertical axis. The maldistribution is not immediately obvious from the overall tracer response curves. Figure 7 illustrates

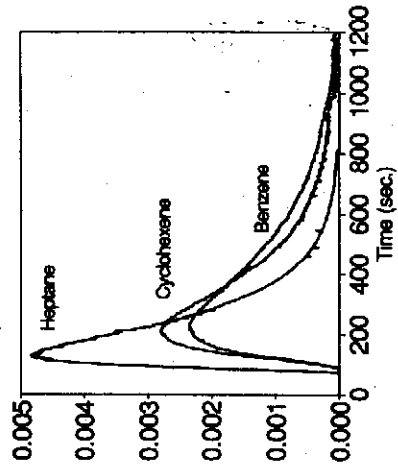


Fig. 7. Impulse responses for three tracers for a tilted column at a liquid flow rate of 0.158 cm<sup>3</sup>/s and a gas flow rate of 3.5 cm<sup>3</sup>/s (STP).

the overall response curves for the three tracers at a liquid flow rate of 0.158 cm<sup>3</sup>/s and a gas flow rate of 3.5 cm<sup>3</sup>/s (at STP). The same response curve (Fig. 5) for the volume external to the reactor bed was valid for this system. The effects of tilting can be seen more dramatically, as illustrated in Fig. 8, by comparing the overall response curve of the tilted bed and the overall response curve of the bed under normal operating conditions for the nonadsorbing tracer, heptane. Notice that, for the tilted column, the peak response time is shifted to an earlier time. This gives, as expected, an indication of gross liquid by-passing. The mass balance requirement (i.e. the area under the curve) indicates that a greater portion of the tracer is in the tail of the response curve for the tilted reactor than for the well-distributed reactor, although this is not obvious from Fig. 7 or 8. The difference in mean residence time in the normal and maldistributed reactor is hence not as great as indicated by the peaks in Fig. 8. One should also note that, in the absence of a tracer response for the "normal operation" as a standard, the overall response of the tracer for the tilted

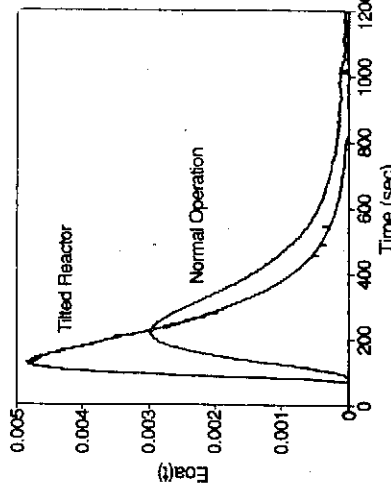


Fig. 8. Comparison of the overall impulse response for the tilted and normal reactor for the nonadsorbing tracer (heptane).

reactor in Figs 7 and 8 give no clear indication of maldistribution.

Figure 9 shows the predicted  $E_{\text{ext}}(t)$  by the LT method from the tracer response curves, shown in Fig. 7, for each of the three tracers. The same particle transfer function [eqs (5)-(8)] and parameters (listed in Tables 1 and 2), as those used for the reactor under normal operating conditions (at the same gas and liquid flow rates), were utilized. The LT method now fails to produce a single  $E_{\text{ext}}(t)$  shape for the three tracers. The mean residence times for the external response curves, and therefore the liquid holdup, are similar for the three tracers: 57.6 s for heptane, 58.3 s for cyclohexene, and 58.6 s for benzene. This corresponds to an external liquid holdup of about 0.12. However, the mean residence time and the external liquid holdup is only slightly smaller (a few percent) for the maldistributed reactor than for the well-distributed one. This indicates that it would be difficult to establish maldistribution in the reactor from calculated values of liquid holdup since these values for the normal and maldistributed cases are so similar. However, maldistribution is indicated by the obvious failure of the LT method to produce a single external fluid impulse response,  $E_{\text{ext}}(t)$ , for all tracers (see Fig. 9). The same bed, the same carrier fluid and the same three tracers were used in the vertical and tilted reactor. At all flow rates, the LT method applied to the vertical reactor tracer data produced a single  $E_{\text{ext}}(t)$  for all tracers as illustrated in Fig. 6. At all flow rates, the LT method, when applied to tracer responses of the maldistributed (tilted) reactor, failed to produce a single  $E_{\text{ext}}(t)$  curve as illustrated in Fig. 9. It is clear that the spread of the curves around the mean in Fig. 9 is tracer dependent. Thus, the failure of the LT method to produce a single  $E_{\text{ext}}(t)$  can be taken as a clear indication of maldistribution.

This conclusion seems at first to contradict our previously reported finding that the LT method, when applied to numerical data with simulated experimental noise, can recover  $E_{\text{ext}}(t)$  for both normal and

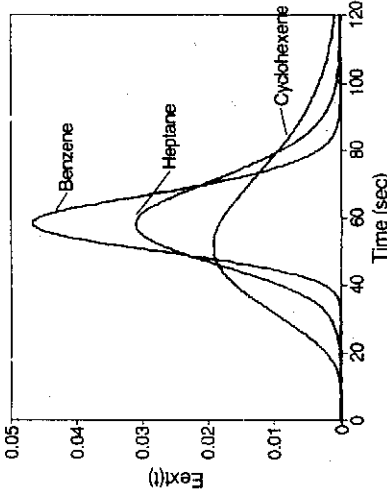


Fig. 9. External impulse response,  $E_{\text{ext}}(t)$ , for the tilted reactor, predicted by the LT method from the responses illustrated in Fig. 7.

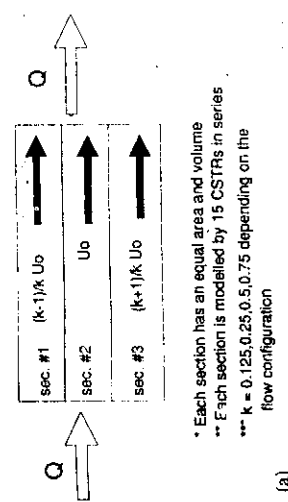
maldistributed reactors (Hanratty and Duduković, 1990). Such computer simulation assumes that the same average particle transfer function is applicable to the whole reactor. This is a good assumption when the flow is well-distributed and local flow rates are close to the average one. In such situations, for well-distributed reactors, the LT method recovers the  $E_{\text{ext}}(t)$  from real data as shown in Fig. 6. In a maldistributed reactor, however, the assumption of a single particle transfer function breaks down. Tilting of the column causes vastly different local liquid flow rates and holdups in different regions of the bed, subjecting particles in these regions to considerably different particle-tracer interactions. Thus, a single particle transfer function,  $H_i(s)$ , whose parameters are evaluated at the mean flow rate, does not any more describe the overall particle-tracer interactions properly in a maldistributed reactor. Therefore, the failure of the LT method to produce a single  $E_{\text{ext}}(t)$  is an indication that the variation in particle transfer functions in the bed is large, which, since particles of uniform properties are used, implies that the flow is maldistributed. The validity of this conclusion is confirmed via computer simulations.

#### COMPUTER SIMULATION

Computer simulation is used to further investigate both the effects of liquid maldistribution upon the LT method and the sensitivity of the method to inaccuracies in the particle model and particle model parameters. The results of this investigation are shown in the following sections.

#### Liquid maldistribution effects

For a maldistributed reactor, different regions of the reactor experience different particle-tracer interaction effects, so that an averaged particle transfer function for the reactor may not be a valid assumption. To test this assertion, reactor tracer responses were generated numerically and analyzed by the LT



(a)

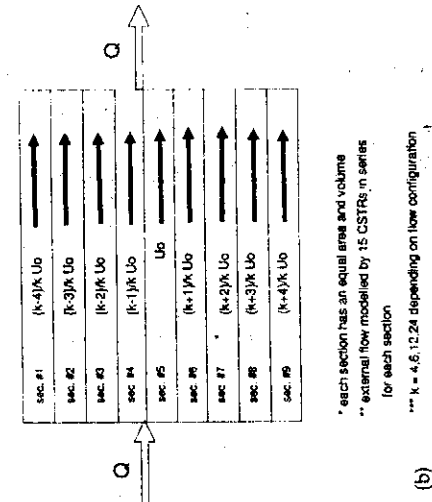


Fig. 10. Two reactor configurations used for computer simulation study.

method for two different reactor configurations with varying degrees of flow maldistribution.

The two simulated reactor configurations are illustrated in Fig. 10. For reactor configuration No. 1, the reactor is split into three distinct flow regions operating in parallel. For reactor configuration No. 2, the reactor is split into nine distinct flow regions operating in parallel. No cross mixing is allowed among different parallel sections. Since reactor configuration No. 2 is modelled by more sections (than No. 1), it more closely approximates a reactor with a smooth radial velocity profile. Since each section of the reactor has a different flow rate, each section has a different mean residence time and different particle-tracer interactions (because of different values for the liquid holdup, mass transfer coefficients, etc.).

To generate the reactor tracer response curves for both reactor configurations, the LT method was applied in reverse order, similar to the procedure described by Hanratty and Duduković (1990). The flow external to the particles in each reactor section was modelled by 15 well-mixed tanks in series (continuously stirred tank reactors) (CSTRs). All reactor sections operate in parallel. In the Laplace domain, the external response curve for each reactor section can be written as

$$\bar{E}_{ext,n}(p) = \frac{1.0}{(r_n p + 1)^{1/3}} \quad (10)$$

where  $r_n$  is the average mean residence time for all  $n$  sections of the reactor,  $r_i$  is the mean residence time for a CSTR in section  $i$ ,  $p$  is the Laplace domain variable, and  $n$  corresponds to the section number within the reactor. Equations (10) and (11) are valid for both reactor configurations with  $n = 3$  for reactor configuration No. 1 and  $n = 9$  for reactor configuration No. 2.

To generate the reactor response curves, the particle transfer function, described by eqs (5)–(8), was used. The values for the particle transfer function parameters are listed in Table 3. The parameters  $k_{LS}$  and  $\varepsilon_L$  are different for each section of the reactor because they are dependent on the liquid flow rate which is different in each section. Since the parameters are different in each section of the reactor, the particle transfer function is also different. To simulate three different tracers, the reactor response curve was generated with three different values for the adsorption equilibrium constant  $K_a$  ( $0.0, 4 \times 10^{-4}, 1 \times 10^{-3} \text{ m}^3/\text{kg}$ ).

For both reactor configurations, the extent of maldistribution was varied by changing the difference between the maximum and minimum flow rates in various branches of the reactor. Table 4 shows the flow configurations (flow rates for each of the sections of the reactor) for both reactor configurations. These flow configurations were chosen so that they roughly correspond for both reactor configurations. The superficial velocity for each section of reactor configuration No. 1 equals the average of the superficial velocities through three of the sections in reactor configuration No. 2.

Reversing the LT method, while utilizing for each section of the reactor a particle transfer function dependent on the liquid flow rate in that section, the reactor response curves were generated. Figure 11 illustrates the reactor response curves for both reactor configurations with  $K = 0$  (nonadsorbing tracer) for the four different flow configurations. These correspond to the curves (the response of a non-adsorbing tracer) which normally would be analyzed to evaluate the reactor flow distribution. Visually inspecting the response curves for reactor configuration No. 1 (three sections), some flow maldistribution is apparent for the 0.5/1.0/1.5 split (case 3). However, at the 0.25/1.0/1.75 split (case 4 which is more maldistributed) the maldistribution is hidden in the tail of the response curve, and therefore it could be overlooked. For reactor configuration No. 2, maldistribution is not visually obvious for any of the different flow configurations of Table 4 since it is often hidden in the tail of the response curve.

The LT method was then applied to the reactor response curves generated for the two reactor configurations and the four flow configurations. The same

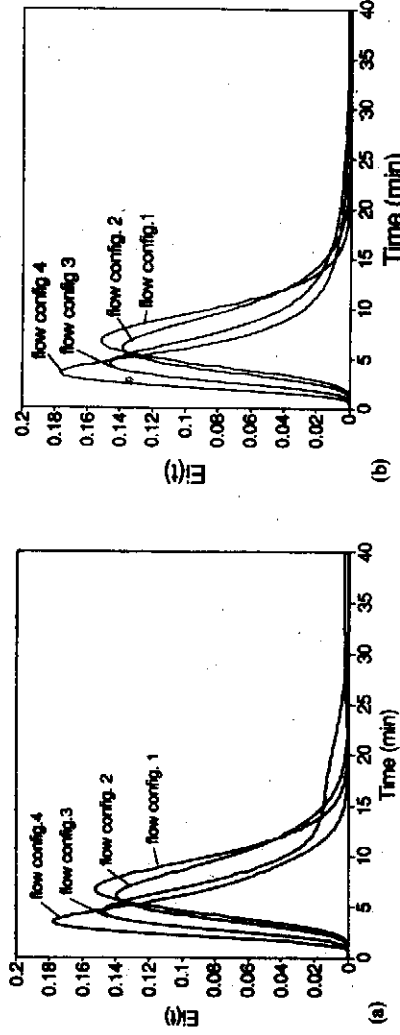
Table 3. Parameters used for computer simulation

Catalyst diameter (m)	$1.6 \times 10^{-3}$
Catalyst density, $\rho_p$ (kg/m <sup>3</sup> )	1250
Catalyst porosity, $\epsilon_p$	0.408
Bed porosity, $\epsilon$	0.54
Liquid holdup, $u_L$	0.174( $u_n/u_{ave}$ ) <sup>0.3441</sup>
Liquid-solid mass transfer coefficient, $k_{L,S}$ (m/s)	$2.5 \times 10^{-5} (u_n/u_{ave})^{0.481}$
Effective diffusivity, $D_{eff}$ (m <sup>2</sup> /s)	$1.06 \times 10^{-9} (u_n/u_{ave})^{0.481}$

<sup>†</sup>n is the section number of the reactor.

Table 4. Flow configurations for computer simulation studies

	Reactor configuration No. 1 ( $u_n/u_{ave}$ for each section)	Reactor configuration No. 2 ( $u_n/u_{ave}$ for each section)
Case No. 1	0.875, 1.0, 1.125	(20, 21, 22, 23, 24, 25, 26, 27, 28)/24
Case No. 2	0.75, 1.0, 1.25	(8, 9, 10, 11, 12, 13, 14, 15, 16)/12
Case No. 3	0.5, 1.0, 1.5	(2, 3, 4, 5, 6, 7, 8, 9, 10)/16
Case No. 4	0.25, 1.0, 1.75	(0, 1, 2, 3, 4, 5, 6, 7, 8)/4

Fig. 11. Tracer response,  $E(t)$ , with  $K = 0$  for all flow distributions and both reactor configurations.

form of the particle transfer function model (that was used to generate the reactor response curves) was utilized. However, now, a single particle transfer function was used. The flow-dependent particle transfer function parameters were assigned values corresponding to the average reactor flow rate (instead of evaluating the transfer function in each section at the local flow rates as was done to generate the response curves in Fig. 11). The other parameters were kept unchanged.

Figure 12(a)-(d) illustrates the external response curves,  $E_{ext}(t)$ , predicted by the LT method for reactor configuration No. 1 for each of the four different flow configurations of Table 4. Figure 12(a) and (b) illustrates that the LT method predicts the external response very well for a reactor which is not much maldistributed. As the maldistribution increases, the LT method begins to falter and instead of predicting a single external response it produces somewhat differ-

ent and incorrect external response curves for the different tracers, as illustrated in Fig. 12(c) and (d).

Figure 13(a)-(d) illustrates the external response curves,  $E_{ext}(t)$ , produced by the LT method for reactor configuration No. 2 for each of the different flow configurations. Again, Fig. 13(a) and (b) illustrates that the LT method predicts the external response very well for a reactor which is not maldistributed. As the maldistribution in the reactor becomes more drastic, the LT method begins to falter and predicts somewhat different and incorrect external response curves for the different tracers, as illustrated in Fig. 13(c) and (d).

The computer simulation results illustrate a number of points. The LT method can predict reasonably the external response curve of a well-distributed or a mildly maldistributed reactor. As the maldistribution becomes more severe, the LT method fails by producing different external responses for the different

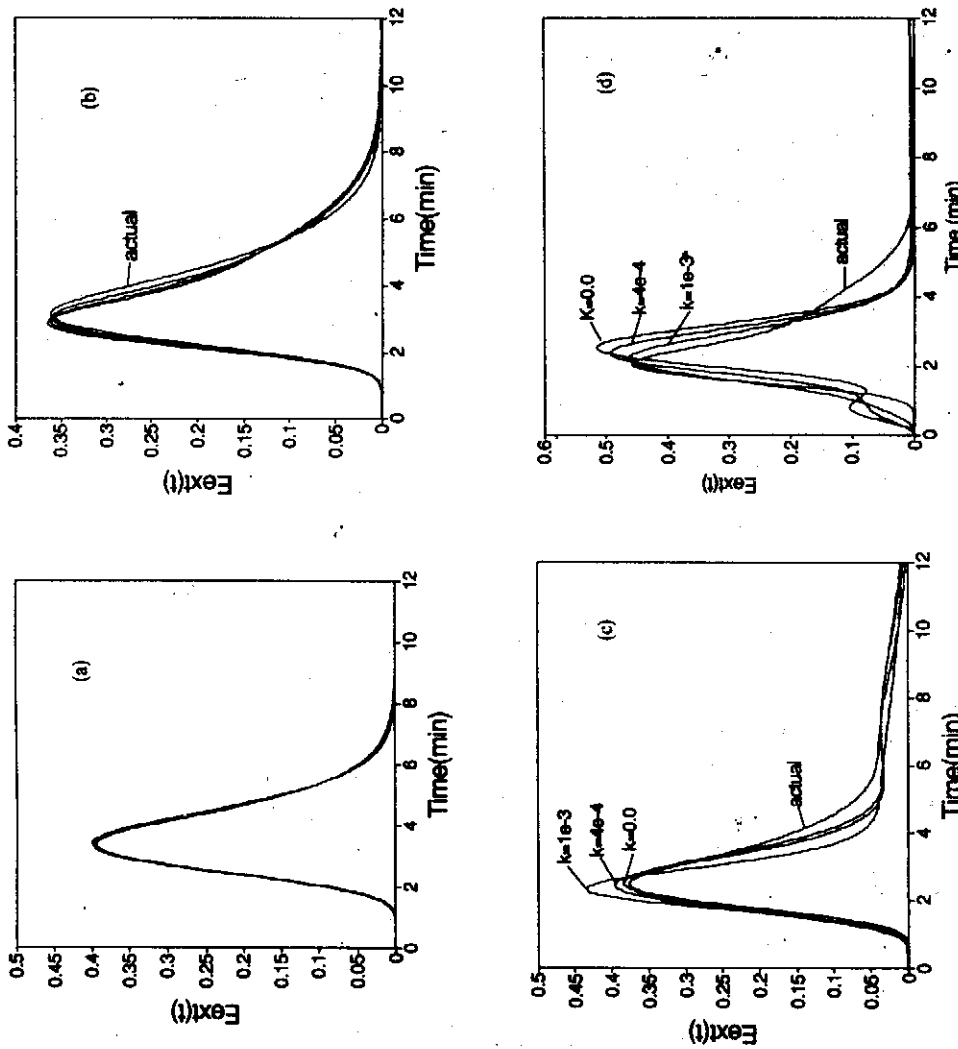


Fig. 12. Predicted external response,  $E_{\text{ext}}(t)$ , for reactor configuration No. 1: (a) flow split 0.75/1.0/1.25, (b) flow split 0.5/1.0/1.5 and (d) flow split 0.25/1.0/1.75.

tracers. Quantification of when the method will fail is not possible from these studies. However, the failure of the LT method to produce a single external response for multiple tracers can be viewed as an indication of gross flow maldistribution as concluded in the previous section. Quantification of maldistribution is not a desirable goal. One simply needs the method to detect it in order to avoid it. The LT method seems capable of that detection task.

One can question whether inaccuracies in the particle transfer function model or in its parameters could cause the LT method to fail even for a well-distributed reactor. In the section that follows, we show that this is not the case.

**Sensitivity of the LT method to particle model and parameter inaccuracies**

The particle transfer function and its parameters are fundamental while applying the LT method. For the particle model, described by eqs (5)-(8), the key parameters are the liquid-solid mass transfer coeffi-

cient ( $k_{LS}$ ), the effective diffusivity ( $D_{eff}$ ) and the adsorption equilibrium constant ( $K_a$ ). Often these parameters (especially the effective diffusivity and the mass transfer coefficient) and the particle model cannot be determined with great accuracy. Therefore, the sensitivity of the LT method to inaccuracies in the particle transfer function model and its parameters was investigated via computer simulation.

Earlier studies (Hamatty, 1988) investigated the sensitivity of the LT method to the particle transfer function formulation and to inaccuracies in the adsorption equilibrium constant. It was shown, by applying the LT method based on a particle transfer function for a sphere to the reactor tracer response curves generated by using particle transfer functions of different assumed particle geometries (such as slab or sphere), that a good representation of the external tracer response curve was obtained whenever a reasonable (but not necessarily exact) particle transfer function model was used. For example, the model for the slab can replace that for a sphere provided the

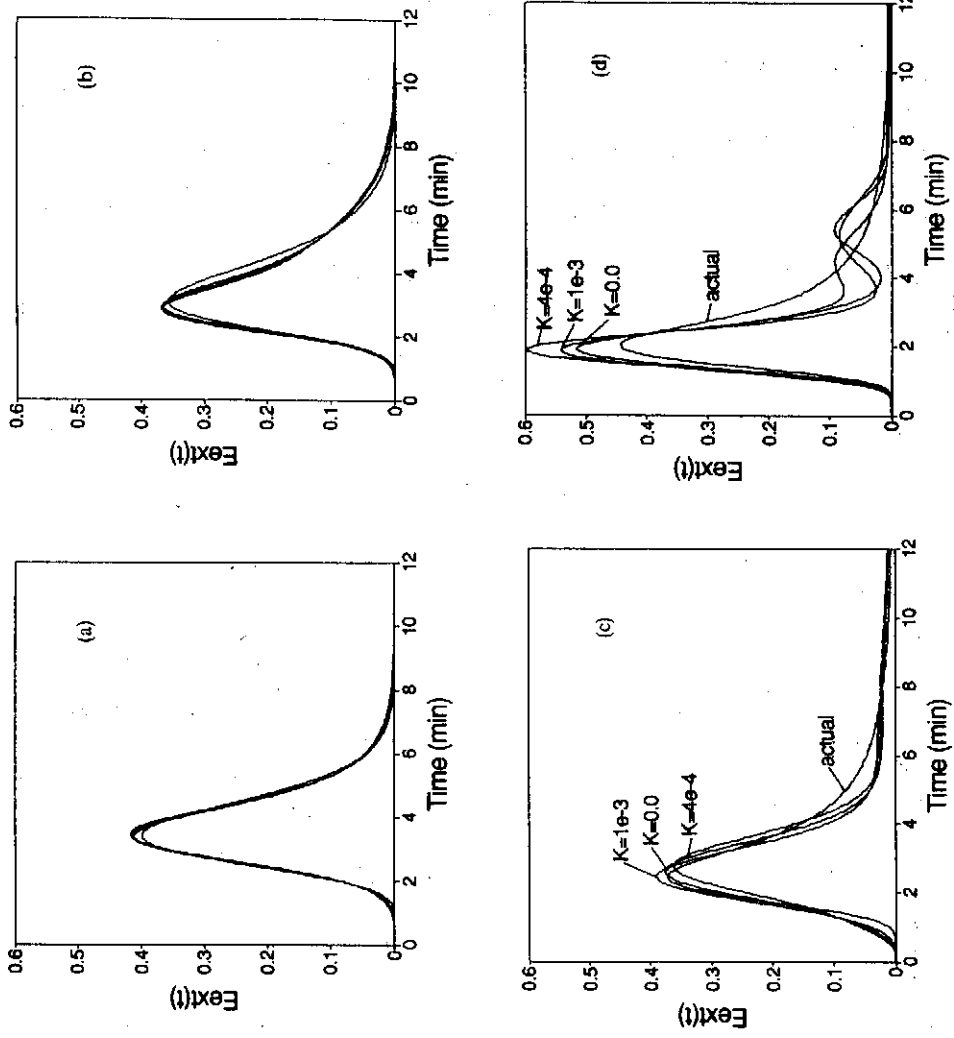


Fig. 13. Predicted external response,  $E_{\text{ext}}(t)$ , for reactor configuration No. 2: (a) flow split (20, ..., 28)/24, (b) flow split (10, ..., 12)/6, (c) flow split (8, ..., 16)/12, and (d) flow split (0, ..., 8)/4.

characteristic diffusion times are the same for the two. The change in the particle model did not adversely affect the LT method as long as the same particle model form was used for all tracers. The effect of inaccuracies in the adsorption equilibrium constant,  $K_a$ , was also investigated.

It was found that if multiple tracers are used, the effects of the inaccuracies could be virtually eliminated if the mean residence time of the predicted external response curves are forced to be equal for all of the tracers. This is a reasonable assumption because the mean residence time of the external tracer response curve should be independent of the tracer. The shape of the external response curve was the same for all tracers even when equilibrium constants for some of them were inaccurate. One should recall that setting the mean of the external response curve to be the same cannot bring the response curves together in a mal-distributed reactor (Fig. 9).

To investigate the effects of inaccuracies in the effective diffusivity and the liquid-solid mass transfer coefficient, overall tracer response curves were gener-

ated in the manner described earlier in this paper. The external response curve was modelled by 15 CSTRs in series and can be described by eq. (11) with  $n = 1$  and  $\tau_{\text{ave}} = \tau_i = 0.5$  min. The particle transfer function described by eqs. (5)-(8) and the parameters listed in Table 3 were utilized to generate the reactor tracer response curves. The LT method was then applied to these curves while using inaccurate values of the effective diffusivity and liquid-solid mass transfer coefficient.

Figure 14 shows the predicted external response curves when the overall tracer response curve is analyzed by the LT method with inaccuracies in the effective diffusivity of  $-20\%$  to  $+50\%$  of its actual value. Clearly, the LT method does not fail and predicts the external response curve well. The same results were obtained if effective diffusivity varied within  $\pm 100\%$ . Figure 15 shows the external response curves predicted by the LT method using a value for  $k_{LS}$  which deviates by  $-20\%$  to  $+50\%$  from its actual value. Again, essentially the same holds good for variation in the liquid mass transfer coeffi-

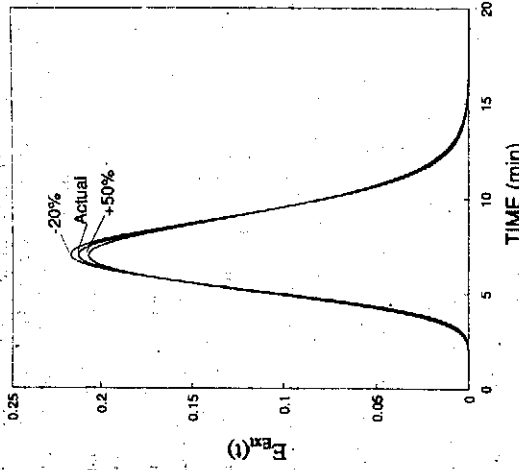


Fig. 14. Predicted external response curves with imposed inaccuracies in the effective diffusivity.

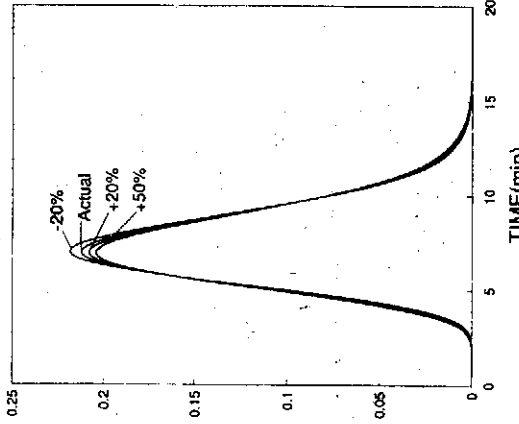


Fig. 15. Predicted external response curves with imposed inaccuracies in the liquid-solid mass transfer coefficients.

cient of  $\pm 100\%$ . Similar results were obtained for a number of different flow configurations.

Our investigations have shown that the LT method is relatively robust in the presence of experimental noise (Hanratty and Duduković, 1990), inaccuracies in the particle transfer function model (Hanratty, 1988), and inaccuracies in the particle transfer function parameter values. The robustness of the LT method supports our contention that the failure of the LT method to produce a single external response curve for multiple tracers of different adsorptivity is an indication of flow maldistribution. This failure is caused by the inability of a single particle transfer function to describe particle-fluid interactions in all regions of a maldistributed reactor.

## CONCLUSIONS

A method by which to decouple the particle-tracer interactions (particle effect) from the tracer response curve of a packed-bed reactor in order to obtain the impulse response of the fluid external to the particles is presented and experimentally confirmed. The resulting impulse response of the external fluid allows for better assessment of the flow distribution in the reactor than the original tracer overall response curve. The method is robust in the presence of reasonable signal noise, particle model formulation inaccuracies and model parameter inaccuracies.

A single particle transfer function is sufficient to describe particle-fluid interactions in a reactor with uniform flow distribution. Thus, for a reactor with no or a small amount of maldistribution the method produces a single impulse tracer response for the fluid external to the particles from the experimentally determined reactor tracer impulse responses for tracers

of different adsorptivity. Departure from plug flow can readily be assessed from the external fluid response obtained.

A single particle transfer function is inadequate to describe particle-fluid interactions in a maldistributed reactor with widely varying regional flow rates. As a consequence, when the LT method, which uses such a single particle transfer function, is applied to tracer impulse responses for tracers of different adsorptivity, it fails to generate a single curve for the impulse response of the fluid external to particles. This failure of the otherwise robust method to generate the external fluid impulse response is caused by, and is therefore an indication of, flow maldistribution.

## NOTATION

- $Bi$  Biot number defined by eq. (6)
- $C_i$  concentration of tracer  $i$ , mol/m $^3$
- $D_{eff}$  effective diffusivity, m $^2$ /s
- $E_i(t)$  overall impulse tracer response for tracer  $i$
- $E_{ext}(t)$  external impulse tracer response
- $E_{obs}(t)$  impulse tracer response of the entire system (reactor + externals)
- $E(s)$  Laplace transform of  $E(t)$
- $H_i(s)$  particle transfer function
- $k_{ex,i}$  mass exchange coefficient, 1/s
- $k_{LS}$  liquid-solid mass transfer coefficient, m/s
- $K_a$  adsorption equilibrium constant, m $^3$ /kg
- $L(\cdot)$  linear operator describing the flow field
- $\mathcal{L}^{-1}$  inverse Laplace operation
- $n$  reactor section number
- $p$  Laplace variable
- $s$  Laplace variable

$S_x$	external particle surface area, $\text{m}^2$
$t$	time, s
$V_p$	particle volume, $\text{m}^3$

**Greek letters**

$\epsilon$	bed porosity
$\epsilon_L$	liquid holdup
$\epsilon_P$	particle porosity
$\eta_{ce}$	external particle wetting efficiency
$\eta_{ci}$	internal particle wetting efficiency
$\rho_p$	particle density, $\text{kg}/\text{m}^3$
$\tau_{ave}$	average mean residence time in the whole reactor in computer simulation studies
$\tau_a$	mean residence time for a single CSTR of section $n$ in computer simulation studies
$\Phi_T$	modified Thiele modulus, defined by eq. (7)
$\Phi_1$	variable defined by eq. (8)

**REFERENCES**

- Aris, R., 1982, Residence time distribution with many reactions in several environments, in *Residence Time Distribution Theory in Chemical Engineering* (Edited by A. Pelet et al.), pp. 23-40. Verlag Chemie, Weinheim.
- Beaudry, E. G., 1987, Modelling of trickle-bed reactors at low liquid flow rates. D.Sc. dissertation, Washington University, St. Louis.
- Beaudry, E. G., Duduković, M. P. and Mills, P. L., 1987, Trickle-bed reactors: liquid diffusion effects in gas-limited reactions. *A.I.Ch.E. J.* **33**(9), 1435-1447.
- Duduković, M. P., 1986, Tracer methods in chemical re-
- actors, techniques and applications, in *Chemical Reactor Design and Technology*. (Edited by H. I. de Lasa), pp. 107-189. NATO ASI Series E—Applied Sciences No. 110. Martinus Nijhoff, Dordrecht.
- Dwivedi, P. N. and Upadhyay, S. N., 1977, Particle-fluid mass transfer in fixed and fluidized beds. *IEC Proc. Des. Dev.* **16**, 157-165.
- El-Hisnawi, A. A., Duduković, M. P. and Mills, P. L., 1982, Dynamic tracer tests, reaction studies and modelling of reactor performance. *ACS Symp. Ser.* **195**, 421-440.
- Hanratty, P. J., 1988, Dynamic modelling of trickle-bed reactors. Masters thesis, Washington University, St. Louis.
- Hanratty, P. J. and Duduković, M. P., 1990, Detection of flow maldistribution in packed-beds via tracers. *A.I.Ch.E. J.* **36**, 127-132.
- Mills, P. L. and Duduković, M. P., 1981, Evaluation of liquid-solid contacting in trickle-bed reactors by tracer methods. *A.I.Ch.E. J.* **27**, 893-904.
- Naor, P. and Shinar, R., 1963, Representation and evaluation of residence time distributions. *IEC Fundam.* **2**, 278-293.
- Ramachandran, P. A. and Smith, J. M., 1982, Effectiveness factors in trickle-bed reactors. *A.I.Ch.E. J.* **28**, 190-195.
- Robinson, B. A. and Tester, J. W., 1986, Characterization of flow maldistribution using inlet-outlet tracer techniques: an application of internal residence time distributions. *Chem. Engng. Sci.* **42**, 469-483.
- Sapre, A. V., Anderson, D. H. and Krambeck, F. J., 1990, Heater probe technique to measure flow maldistribution in large scale trickle-bed reactors. *Chem. Engng. Sci.* **45**, 2263-2268.
- Schneider, P. and Smith, J. M., 1968, Adsorption rate constants from chromatography. *A.I.Ch.E. J.* **14**, 762-771.
- Tan, C. S. and Smith, J. M., 1982, A dynamic method for liquid particle mass transfer in trickle-bed reactors. *A.I.Ch.E. J.* **28**, 145-190.